Journal of Applied Polymer Science

Influence of the coagulation medium on the performance of poly(ether sulfone) flat-sheet membranes

Martin Spruck,[1] Werner Stadlmayr,[1] Marc Koch,[1] Lukas Mayr,[2] Simon Penner,[2] Marco Rupprich[1]

[1]Department of Environmental, Process, and Energy Engineering, Management Center Innsbruck–The Entrepreneurial School, Maximilianstrasse 2, Innsbruck 6020, Austria

[2]Institute of Physical Chemistry, University of Innsbruck, Innrain 80-82, Innsbruck 6020, Austria

Correspondence to: M. Rupprich (E-mail: marco.rupprich@mci.edu)

ABSTRACT: Poly(ether sulfone) flat-sheet membranes were fabricated via phase inversion with different nonsolvent mixtures. The effect of the nonsolvent water with the addition of various amounts of ethanol, acetone, or isopropyl alcohol on the membrane morphology (as measured with scanning electron microscopy and atomic force microscopy) and the filtration performance were investigated. For the statistical evaluation of the fabrication process, on average, six membranes were produced. The pure water flux (PWF) and macromolecule retention were determined via filtration experiments. The presence of coagulation additives resulted in modified precipitation kinetics and thermodynamics, yielded different membrane structures, and therefore, influenced the performance. The results show that the addition of ethanol, acetone, and isopropyl alcohol in low concentrations (up to 10%) to water led to an increasing PWF. Higher concentrations led to a decrease in PWF. For high concentrations (>30%), a change in the membrane morphology from fingerlike to spongelike structures was expected, and this was experimentally proven for the case of ethanol. One main finding was the similarity of the influence of the used additives on the membrane performance. This was to be expected from Flory–Huggins theory for additives with high water miscibility; hence, under these circumstances, entropic and not energetic reasoning dominated the phase-inversion process. © 2014 Wiley Periodicals, Inc. J. Appl. Polym. Sci. **2015**, *132*, 41645.

KEYWORDS: manufacturing; membranes; morphology; separation techniques

Received 22 April 2014; accepted 16 October 2014

DOI: 10.1002/app.41645

INTRODUCTION

Compared to thermal separation techniques, the advantages of membrane technology are lower energy consumption and performance within a wide temperature range. Since the preparation of the first asymmetric polymer membranes via phase inversion by Loeb and Sourirajan,[1] a lot of research has been done in this field.[2] In the phase-inversion process, a casting solution of a polymer, dissolved in an appropriate solvent, is immersed into a coagulation bath containing a nonsolvent.[3] The formation of different membrane structures is controlled by the kinetics of the transport process and the thermodynamics of the casting solution.[4] The immersion of the polymer dope into a coagulation bath leads to diffusional interchange between the solution and the nonsolvent.[5] The solvent diffuses into the coagulation bath, whereas the diffusion of the nonsolvent into the polymer film takes place. It is possible to diversify formed membranes from applications for microfiltration to reverse osmosis by changing several parameters during the inversion process.[2] Pressure-driven separation techniques (e.g., microfiltration, ultrafiltration, nanofiltration, reverse osmosis) use membranes with an asymmetric structure. A thin porous or nonporous selective layer acts as an active membrane and is on top of a highly porous substructure (thickness = 100–300 μm); this provides sufficient mechanical stability. The transport resistance of an asymmetric membrane is lower compared to symmetric membranes and results in increased membrane permeability. For high-performance membranes, it is necessary to produce the thinnest top layer possible with an effectual support layer.[6] A method for improving the performance of poly(ether sulfone) (PES) membranes is the introduction of additives such as polyvinylpyrrolidone (PVP) or poly(ethylene glycol) into the polymer solution. There are several studies that clearly show that the permeate flux increased with the addition of PVP.[7–9] The type of nonsolvent used is another important factor; this affects the membrane morphology and performance.[10,11] Moradihamedani *et al.*[12] investigated the effect of an addition of 20% ethanol, propanol, or butanol to the nonsolvent and found that the morphology and performance of polysulfone gas-permeation membranes was swayed by the type of organic nonsolvent additive. Iqbal *et al.*[13] studied the formation of asymmetric polycarbonate membranes for CO_2 and CH_4 separation. They compared the effect of three different nonsolvents

Table I. List of Chemicals Used

Name	Grade	Supplier
Ethanol	≥96%	Carl-Roth
Acetone	≥99.5%	VWR International
Isopropyl alcohol	≥99.5%	Carl-Roth
PES	Gafone PES 3100	Solvay Advanced Polymers
PVP	M_w = 29,000, powder	Sigma-Aldrich
DMAc	Puriss, P.A., ≥99.5%	Sigma-Aldrich
Dextran	500 kDa	Sigma-Aldrich

(ethanol, propanol, and butanol) on the membrane structure and separation performance. The results show that addition of butanol produced a highly porous substructure, whereas ethanol resulted in membranes with a less porous substructure.

When the polymer solution is in contact with a coagulation bath containing nonsolvent, a demixing process starts. This demixing can be instantaneous or delayed for a certain period of time. In the case of delayed demixing, membranes without macrovoids are the result of the formation process, whereas membranes with macrovoids are formed in the case of instantaneous demixing.[14]

The main objective of this study was to present results showing the effects of different coagulation bath additives, with all other influencing parameters such as the temperature remaining constant, on the performance of PES flat-sheet membranes fabricated via phase inversion.

The results show that the phase-inversion process and the performance of the formed membranes were strongly influenced by the coagulation bath mixture. An addition of ethanol, acetone, or isopropyl alcohol to the classical nonsolvent water leads to complex behavior of the pure water flux (PWF), with an initial rise for additive concentrations up to 10%; this is independent of the chemical nature of the nonsolvent additives used. With higher amounts, a decreasing PWF was observed. Thermodynamic considerations were applied to explain said behavior. Additionally, the obtained results were compared to recent results for gas-permeation membranes based on PES.[12,15]

EXPERIMENTAL

Materials

Polymer solutions were prepared with PES (Gafone PES 3100) from Solvay Advanced Polymers, PVP (powder, M_w = 29,000) from Sigma-Aldrich as the pore-forming polymer additive, and *N,N*-dimethylacetamide (DMAc; Puriss, P.A., ≥99.5%) from Sigma-Aldrich as the solvent. For macromolecular retention investigations, dextran with an average molecular weight of 500 kDa was supplied by Sigma-Aldrich. As coagulation bath additives, ethanol (≥96%) by Carl-Roth, acetone (≥99.5%) obtained from VWR International, and isopropyl alcohol (≥99.5%) from Carl-Roth were used. All of the chemicals were used without any further purification (Table I). Deionized water was used as the nonsolvent.

Fabrication of the PES Flat-Sheet Membranes

A concentration of 17% PES was dissolved in DMAc. As a pore-forming polymer additive, 4 wt % PVP was added to every casting solution. The PES and PVP powders were dried for at least 6 h at 60°C in a drying oven before use. To ensure the complete solution of the polymer and additive, the dopes were mixed for 20 h in an overhead shaker at room temperature. The dope solutions were degased for 2 h before membrane fabrication. To produce flat-sheet membranes, a 200-μm thin film of the polymer solution was cast onto a glass plate. The system was immersed directly into a coagulation bath containing different coagulant mixtures. After 5 min in the first bath, the membranes were taken out and immersed for 24 h in a second bath containing the same coagulant fractions.

To prevent changes in the precipitation kinetics caused by temperature changes, the temperature of the coagulant composition was adjusted to 20 ± 1°C for every membrane. The mixtures of the coagulation bath are shown in Table II.

Viscosity Measurement

The shear viscosity values of the PES/PVP–DMAc solutions were measured as a function of the PES concentration at a constant shear rate of 100 s^{-1} and a temperature of 20°C. As the operation system, an Anton Paar Rheolab QC (CC27) rotational viscometer was used.

Cloud-Point Measurement

Cloud points of different coagulant media were determined by a rapid titration method described by Wijmans *et al.*[16] The cloud-point composition was calculated by the amounts of added coagulant and primary polymer solution. In the case of two

Table II. Coagulation Bath Compositions of Formed Membranes

Membrane	Coagulation bath	Ratio
W100	Water	100
W98E2	Water/ethanol	98:2
W96E4	Water/ethanol	96:4
W94E6	Water/ethanol	94:6
W92E8	Water/ethanol	92:8
W90E10	Water/ethanol	90:10
W85E15	Water/ethanol	85:15
W80E20	Water/ethanol	80:20
W70E30	Water/ethanol	70:30
W50E50	Water/ethanol	50:50
W98I2	Water/isopropyl alcohol	98:2
W96I4	Water/isopropyl alcohol	96:4
W94I6	Water/isopropyl alcohol	94:6
W92I8	Water/isopropyl alcohol	92:8
W90I10	Water/isopropyl alcohol	90:10
W85I15	Water/isopropyl alcohol	85:15
W90A10	Water/acetone	90:10
W70A30	Water/acetone	70:30

Systematic nomenclature is as follows: letters denote components (W: water, E: ethanol, I: isopropyl alcohol, A: acetone); numbers denote composition in percent (w/w).

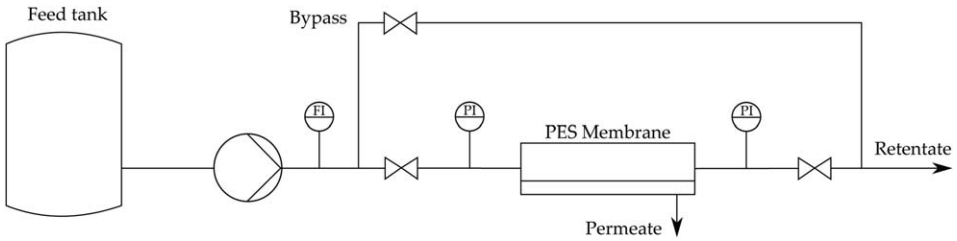

Figure 1. Schematic flow diagram of the test device.

coagulants, the polymer solution was titrated with a mixture of water and additives.

Characterization of the Fabricated Flat-Sheet Membranes Morphology [Scanning Electron Microscopy (SEM) and Atomic Force Microscopy (AFM)]. The cross-sectional morphology of all of the fabricated flat-sheet membranes was investigated with SEM (JEOL, NeoScope, JCM-5000). The membrane samples were dried at 60°C for 24 h before they were immersed and fractured in liquid nitrogen.

As Shirazi and coworkers[17,18] pointed out, AFM is a useful tool for studying the surface topography of the membranes. Thus, AFM analysis was performed with a Veeco Instruments Dimension 3100 atomic force microscope with a Nanoscope IVa controller and a vibration isolation system under ambient conditions. The microfabricated probes of phosphorous-doped silicon with cantilever resonance frequencies of around 300 kHz and a spring constant of around 50 N/m were used. The AFM was operated in tapping mode at room temperature in air. Scans of 10 × 10 or 5 × 5 μm^2 were thereby recorded. The topographical data, amplitude, and phase signals were recorded simultaneously. From the topographical data, the first-order plane fit was subtracted.

Water Flux. Figure 1 shows the schematic flow diagram of the membrane testing unit. For measurement of the PWF, tap water with a temperature of 25°C and a transmembrane pressure of 0.1 MPa was used for all of the experiments. The membrane cell for rectangular flat sheets had an effective area of 0.008 m^2.

Macromolecular Retention. Solutions of tap water and dextran (0.085 wt %) were used as feed for the filtration experiments. The feed temperature was 25°C for all of the rejection investigations. To calculate the separation efficiency, dextran with a molecular weight of 500 kDa was used. The percentage dextran rejection [R (%)] was calculated with the following equation:

$$R(\%) = \left(1 - C_p/C_f\right) \times 100 \quad (1)$$

where C_p is the permeate concentration (mg/L) and C_f represents the feed concentration (mg/L). The dextran concentrations were measured by a TOC–VCPN analyzer from Shimadzu (Total Organic Carbon–V-Series; CPN stands for the oxidation method (combustion), the control method (PC) and the sensitivity (normal) of the analyzer)

RESULTS AND DISCUSSION

Viscosity Analysis

It is shown in Figure 2 that dope viscosity increased rapidly at a level above 21% PES. Wang *et al.*[19] found out that the polymer dope viscosity for flat-sheet membrane preparation should have been at a level of a few hundred milli-Pascal seconds. A higher dope solution viscosity resulted in denser membrane morphology and a decrease in the water flux.[20]

SEM Analysis

Figure 3 shows the cross-sectional SEM images of the membranes prepared with different organic contents in the coagulation bath. The top layer (air side) for all of the SEM images is at the right. The membranes, which were formed via phase inversion, were asymmetric; they consisted of layers with different structures. The morphology showed long and wide but also thin fingerlike pores, fingerlike cavities, macrovoids, and spongelike and dense structures. According to Kesting,[21] membranes with large fingerlike macrovoids and cavities are the result of fast precipitation, whereas slow precipitation forms a spongelike structure. Mulder *et al.*[22] found out that an increase in the polymer concentration resulted in an increase of the top-layer thickness. The viscosity of the polymer dope had an effect on the kinetics of the phase-inversion process.

As the ethanol concentration in the coagulation bath was increased to 50%, the structure changed from fingerlike pores and cavities to a spongelike structure with a denser surface. The photographs in Figure 3 indicate that higher amounts of ethanol and acetone in the coagulation bath led to less porous substructures. When the concentration of ethanol was increased, denser sublayers were formed.

Membranes formed in a coagulation medium containing 10% acetone showed a structure with large cavities in the sublayer. As the acetone concentration was increased to 30%, structures in the sublayer changed to smaller voids, whereas the top layer became less porous.

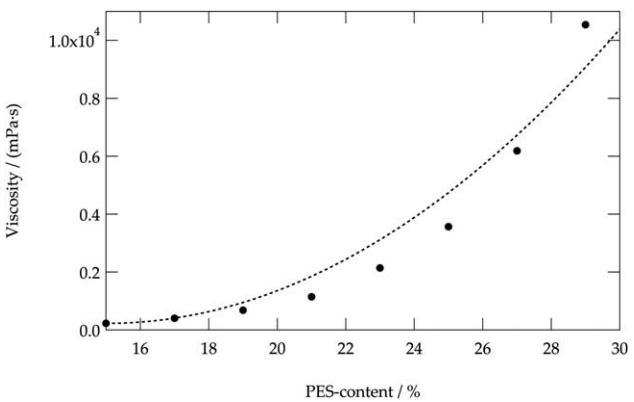

Figure 2. Measured viscosity of the polymer dope solution.

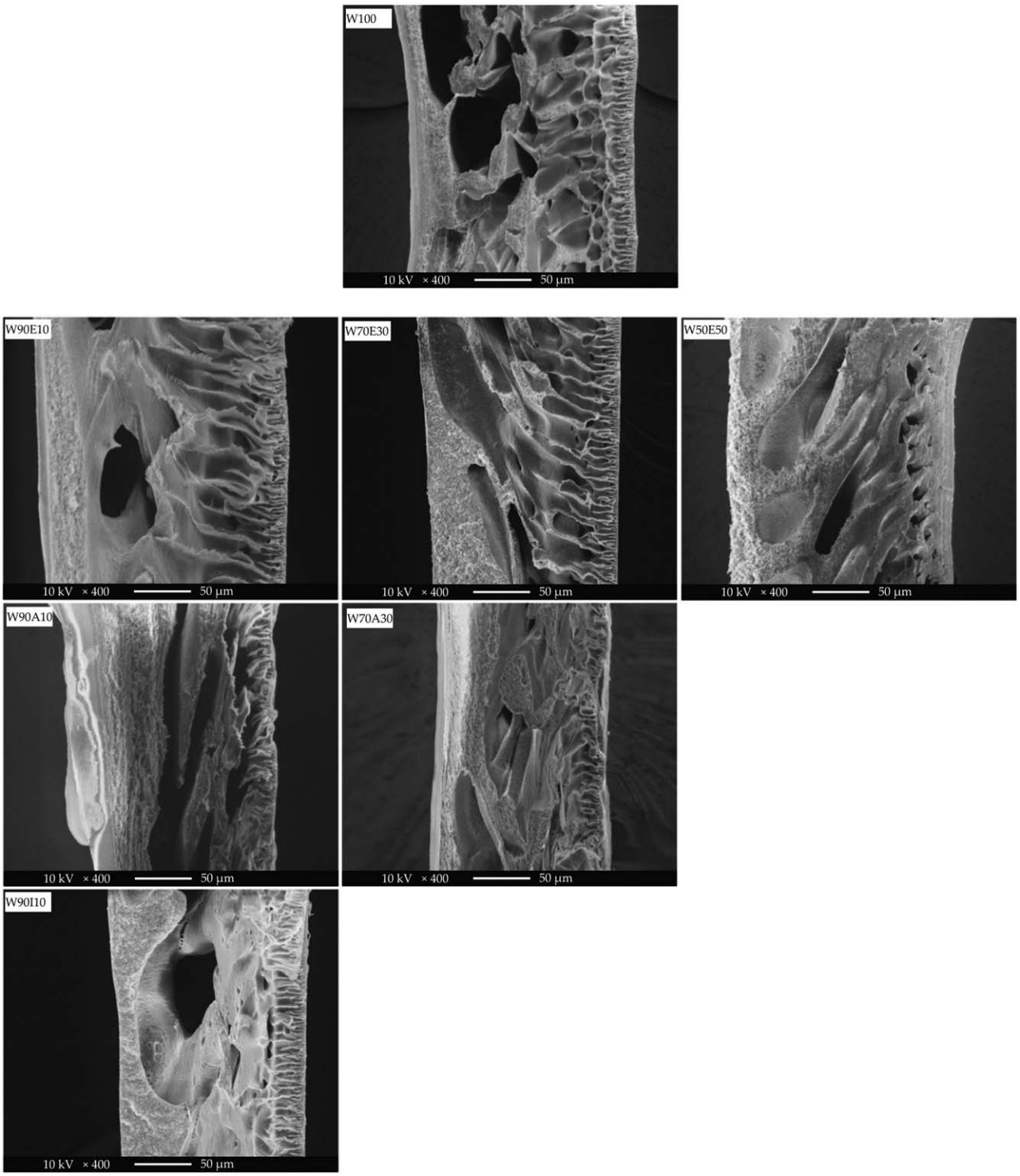

Figure 3. SEM images of the fabricated membranes.

AFM Analysis

As shown in Figure 4, there was no clear trend in the roughness with increasing ethanol content. The root mean square roughness (R_q) values were all in the range between 15 and 35 nm. However, a trend toward anisotropic, more ordered surface was seen. Thus, for illustration purposes, a larger area (10 × 10 μm^2) is shown in a two-dimensional plot, where the periodicity is clearly visible (see Figure 5). The same distance of roughly 5 µm was also unequivocally observed in the samples prepared with 10 and 30% ethanol in the nonsolvent (not shown). However, for concentrations below 10% ethanol, this effect was not observed (e.g., Figure 6). This was reasonable from the thermodynamic point of view because, for increasing ethanol content, delayed demixing was expected. This should have resulted in an

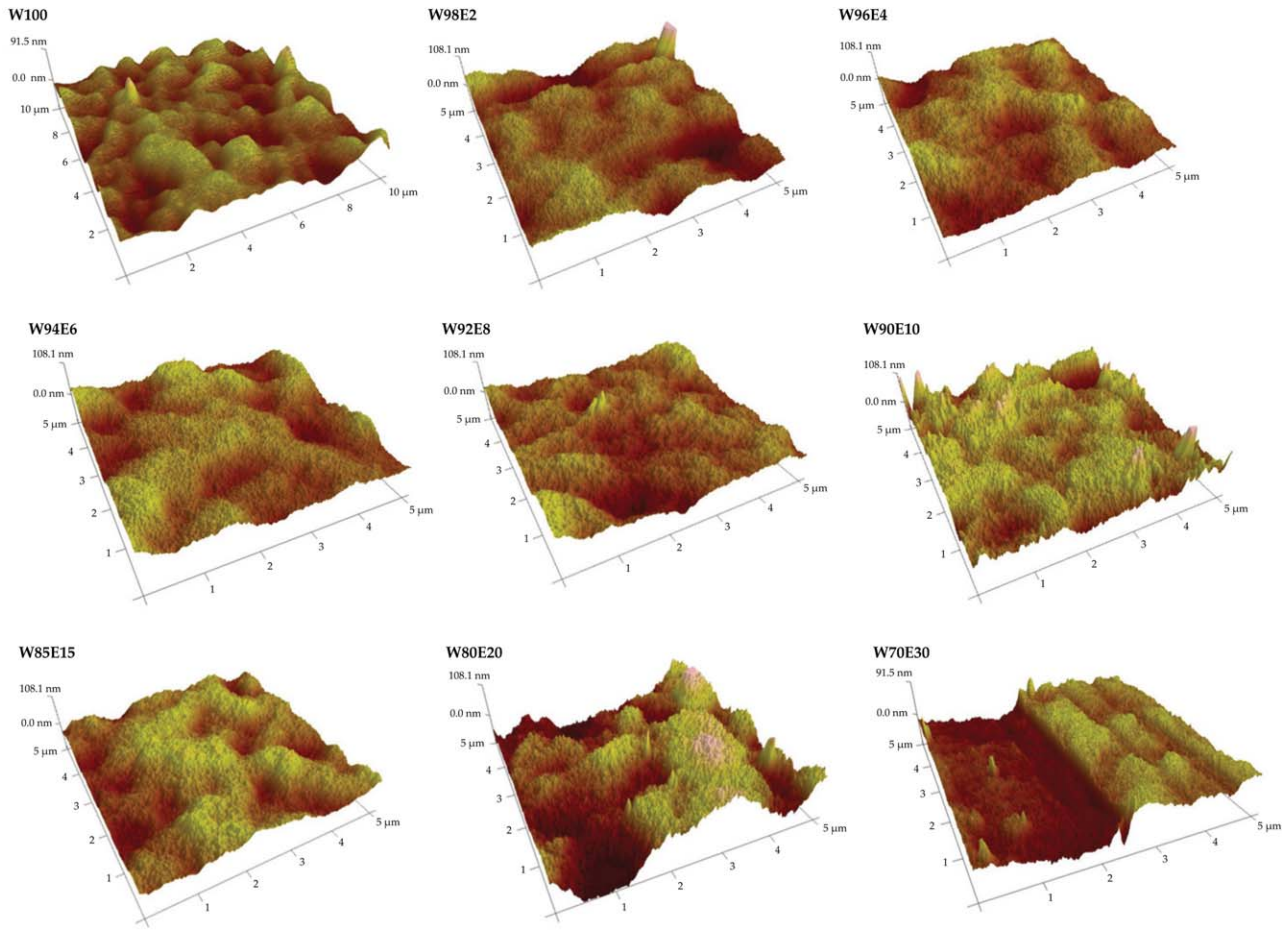

Figure 4. Three-dimensional AFM images of the produced membranes. [Color figure can be viewed in the online issue, which is available at wileyonlinelibrary.com.]

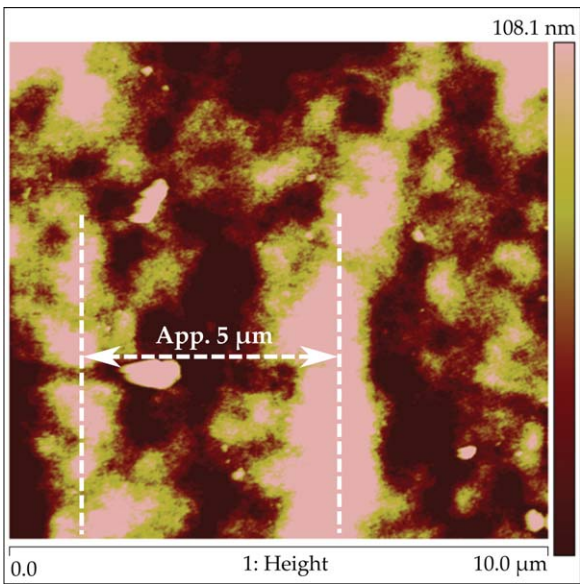

Figure 5. Two-dimensional AFM image of W80E20. The periodicity of the ensuing pattern was approximately 5 µm. App.: approximately. [Color figure can be viewed in the online issue, which is available at wileyonlinelibrary.com.]

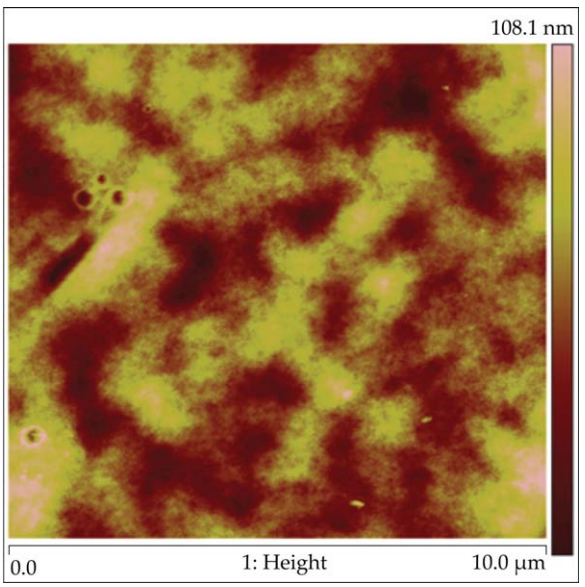

Figure 6. Two-dimensional AFM image of W96E4. No anisotropy was observed. [Color figure can be viewed in the online issue, which is available at wileyonlinelibrary.com.]

Table III. Solubility Parameters and Their Differences

Component	Solubility parameter $(MPa)^{1/2}$				
	δ_d	δ_p	δ_h	$\Delta\delta_{S-NS}$	$\Delta\delta_{P-NS}$
PES	19.6	10.8	9.2	3.1	0.0
Water	15.6	16.0	42.3	32.4	33.7
Ethanol	15.8	8.8	19.4	9.6	11.1
Acetone	15.5	10.4	7.0	3.6	4.7
DMAc	16.8	11.5	10.2	0.0	3.1
Isopropyl alcohol	15.8	6.1	16.4	8.3	9.4
Water/ethanol (90:10)	15.6	15.3	40.0	30.1	31.4
Water/ethanol (70:30)	15.7	13.8	35.4	25.4	26.7
Water/ethanol (50:50)	15.7	12.4	30.9	20.7	22.1
Water/acetone (90:10)	15.6	15.4	38.8	28.9	30.2
Water/acetone (70:30)	15.6	14.3	31.7	21.7	23.1
Water/isopropyl alcohol (90:10)	15.6	15.0	39.7	29.7	31.1

Adapted from ref. 27.

energetically more stable system, presumably with a higher anisotropy.

Cloud Points

Cloud-point experiments were only undertaken with ethanol and acetone because isopropyl alcohol was expected to behave similarly to ethanol because of the solubility coefficient (see Table III). The results in Figure 7 show that the cloud points moved to the polymer–nonsolvent axis when the amount of nonsolvent in the coagulant mixture decreased. Water is a strong nonsolvent for PES, with poor polymer interaction. The demixing gap was diminished for systems containing higher amounts of ethanol or acetone in the coagulation bath. Chun *et al.*[11] pointed out that systems containing solvent in the coagulation medium became thermodynamically more stable. Similar behaviors were observed in systems containing ethanol and acetone. According to Mulder *et al.*,[22] the binodal curve position affects the type of phase separation. A smaller demixing gap can increase delayed demixing processes and produce a dense membrane structure. In other words, more coagulant (i.e., nonsolvent) is needed to enter the unstable region, where phase separation takes place. Therefore, more coagulant has to diffuse into the polymer solution, whereby the tendency of instantaneous demixing is reduced.

As shown in Figure 3, when the ethanol content in the coagulation bath was increased to 50%, the formed membrane had a less porous top layer supported by a dense sublayer. On the basis of the analyses of the cloud-point position, we concluded that the period of time before phase inversion was completed at

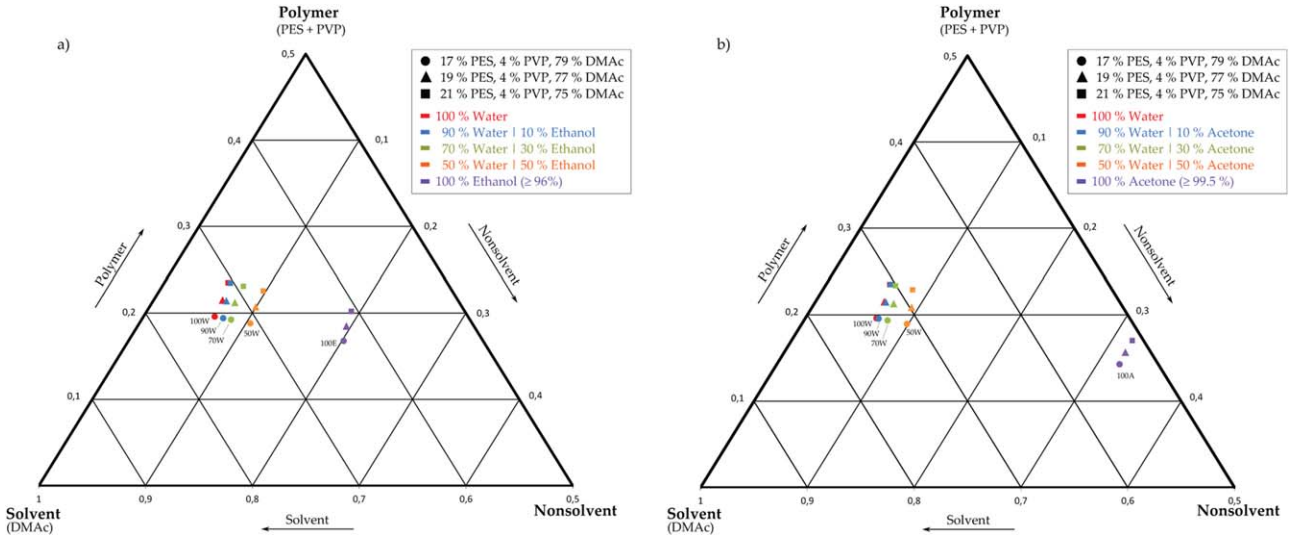

Figure 7. Ternary diagrams of the polymer (PES/PVP), solvent (DMAc), and different nonsolvent mixtures: (a) water and ethanol and (b) water and acetone. [Color figure can be viewed in the online issue, which is available at wileyonlinelibrary.com.]

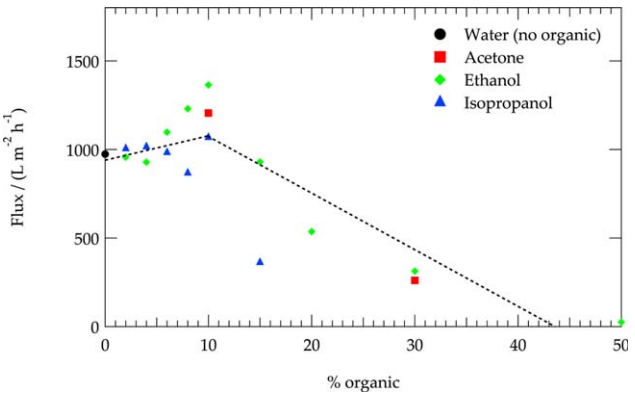

Figure 8. PWF of the membranes produced in different coagulant mixtures (0.1 MPa). The dashed lines are intended to be guides for the eyes. [Color figure can be viewed in the online issue, which is available at wileyonlinelibrary.com.]

$t_{50\%water} > t_{70\%water} > t_{90\%water} > t_{100\%water}$. When the amount of additive in the coagulation bath was increased, the driving force for water diffusion into the polymer solution was reduced. As a result, more time was needed for the phase transition, and delayed demixing was promoted. Similar behavior can be found in the literature.[23–25]

Effect of the Coagulation Bath Mixture on the Water Flux

Figure 8 shows the PWF of the prepared flat-sheet membranes. To obtain the representative data for each coagulation bath mixture, on average, six membranes were prepared and tested. One outlier was detected via the Dean–Dixon testing method. The PWF results showed that addition of up to 10% ethanol, 10% acetone, and 10% isopropyl alcohol led to an increase in the water flux (however, this effect was more prominent for acetone and ethanol), whereas a further increase in organic additive in the bath led to a drastic reduction in PWF. These findings were consistent with SEM studies of the membranes (see Figure 3). This increase in the additive concentration in the coagulation medium resulted in slower precipitation rates; this influenced the morphology and, therefore, the membrane performance. Mulder[26] showed that an increasing content of solvent in the coagulation bath led to a decrease in the polymer concentration at the polymer solution/coagulant interface. As a result of the reduced interfacial polymer concentration, a more porous top layer was formed. This reasoning should have also held true when the water was diluted by a weakly interacting component such as ethanol, acetone, or isopropyl alcohol (see Thermodynamic Considerations section for more information).

Ultrafiltration Experiments

Although macromolecular parameters such as shape and flexibility have to be taken into account, cutoff values are often used in industrial membrane assessment. Figure 9 shows the dextran retention of membranes precipitated in different coagulation media. For the macromolecular rejection test, a minimum PWF of 50 L m^{-2} h^{-1} was defined. The results reveal that the addition of organic additive to water in the coagulation bath had a negative effect on the retention. The solute retention measurements were in accordance with the PWF experiments, with the effect that higher flux led to a decrease in the macromolecule rejection below 10% organic additive. Consequently, these results indicate a high rejection for the membranes prepared with an increased amount of additive in the coagulation bath. Ultrafiltration experiments made with membranes containing, for example, 20% ethanol in the water bath did not confirm this expected trend, but instead, they led to a reduced retention rate of 43%. These result shows that the structural changes of flat-sheet membranes caused by a delayed onset of liquid–liquid demixing led to a decrease in the membrane performance parameter PWF and macromolecular rejection. With the pore flow model taken as a basis, this indicated that the amount of additive influenced the number and size of the membrane pores.

Thermodynamic Considerations

The solubility parameters of the polymer (δ_P), solvent (δ_S), and nonsolvent (δ_{NS}) played a role in membrane formation. Mulder[26] described the solubility parameter theory to give a qualitative model for interactions between polymer, solvent, and nonsolvent. The difference in the solubility between the solvent and nonsolvent is represented by $\Delta\delta_{S-NS}$, and the difference in the solubility between the polymer and nonsolvent is represented by $\Delta\delta_{P-NS}$. The parameters of various coagulation bath compositions were calculated on the basis of the simple additive rule. The solubility parameters of PES, water, ethanol, acetone, isopropyl alcohol, and DMAc, respectively, were obtained from Hansen:[27]

$$\Delta\delta_{S-NS} = \left[\left(\delta_{d,S} - \delta_{d,NS}\right)^2 + \left(\delta_{p,S} - \delta_{p,NS}\right)^2 + \left(\delta_{h,S} - \delta_{h,NS}\right)^2\right]^{0,5} \quad (2)$$

$$\Delta\delta_{P-NS} = \left[\left(\delta_{d,P} - \delta_{d,NS}\right)^2 + \left(\delta_{p,P} - \delta_{p,NS}\right)^2 + \left(\delta_{h,P} - \delta_{h,NS}\right)^2\right]^{0,5} \quad (3)$$

where δ_d is the solubility parameter of diffusion, δ_p is the polar solubility parameter, and δ_h is the solubility parameter of hydrogen. The calculated solubility parameter values for different coagulation bath mixtures and their differences are shown in Table III. The $\Delta\delta_{S-NS}$ and $\Delta\delta_{P-NS}$ values decreased with increasing amount of organic solvent in the coagulation

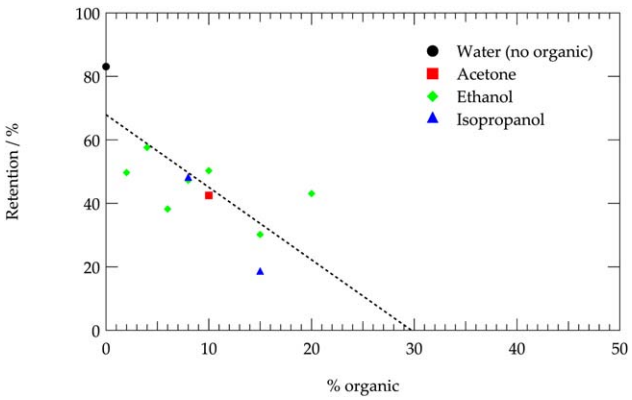

Figure 9. Dextran (500-kDa) retention of the membranes produced in different coagulant mixtures. The dashed line is intended to be a guide to the eye. [Color figure can be viewed in the online issue, which is available at wileyonlinelibrary.com.]

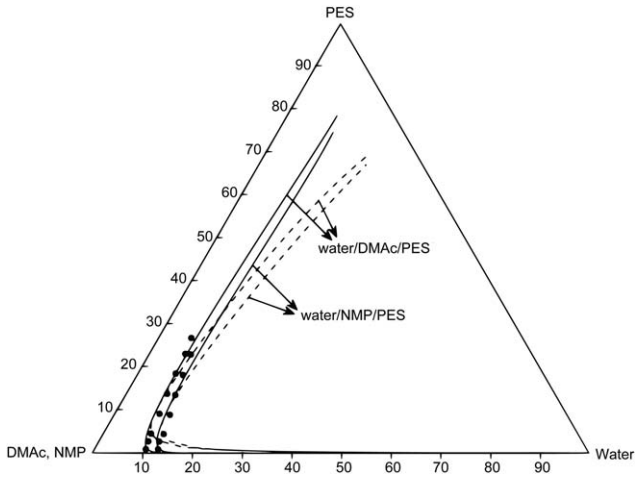

Figure 10. Ternary phase diagram. The solid lines are the binodal curves; the dashed lines the spinodal curves. The dots are points deduced from the cloud-point experiments. Reprinted with permission from ref. 30. Copyright 2008 Elsevier. NMP: *N*-methyl pyrrolidone.

medium. For example, the data showed a decrease in $\Delta\delta_{S-NS}$ from 32.4 to 20.7 $MPa^{1/2}$ with an increasing proportion of ethanol from 0 to 50%.

According to Reuvers,[28] the interaction between the solvent and nonsolvent is an important factor for the formed membrane structure. Chun *et al.*[11] found out that membranes had a lower porosity for decreasing solubility parameters $\Delta\delta_{S-NS}$ and $\Delta\delta_{P-NS}$. The addition of substances with low solubility parameters to a coagulation bath containing water modified the diffusional exchange rates of the solvent and nonsolvent. The addition of solvent to a coagulation bath decreased the $\Delta\delta_{S-NS}$ value, and delayed demixing was promoted. The same effect was expected for any miscible organic solvents. The delayed onset of liquid–liquid demixing indicated that the membrane was not formed immediately after immersion into the nonsolvent bath. According to Wang *et al.*,[29] strong interactions between the polymer and nonsolvent and, therefore, small $\Delta\delta_{P-NS}$ had an effect on the formation of membranes and led to a denser skin layer. SEM images (Figure 3) of the cross section indicated that higher amounts of additives in the coagulation bath resulted in membranes with less porous sublayers.

The results of the experiments shown in Figure 8 could be rationalized in a thermodynamic way. In Figure 10, the ternary phase diagram of water/DMAc/PES was calculated by Barzin and Sadatnia.[30]

With a system without any organic additives taken into account, the starting point was at the DMAc/PES axis at 17% PES. When the polymer-rich phase was followed through the phase diagram, this correlated to movement to a point on the water/PES axis somewhere close to the PES side. The demixing was expected to be instantaneous when the bottom–top path intersected the binodal at the same point (see Figure 11, left side). When the content of organic additive was increased, the drastic decrease in flux shown in Figure 8, around a 10% content of organic solvent (ethanol, isopropyl alcohol, or acetone, respectively), could be explained via the following argumentation.

As calculated by Barzin and Sadatnia,[30] the interaction parameter between the nonsolvent and solvent was dependent on the concentration of water. Ignoring the interaction between organic additives and the other components and only attributing for the effect of dilution of the water, we observed that the parameter rose with decreasing water content (i.e., increasing organic content). As shown in an in-depth study of the phase diagram,[31] this resulted in a shift of the binodal (and presumably also the spinodal) curve to the right (see Figure 11, right side). This was verified by the cloud-point measurements shown in Figure 7.

Thus, the mixing changed from instantaneous to delayed mixing because the path (if it was thought of as constant in the nonorganic and organic cases) was, at some point, no longer crossing the binodal curve but rather approaching, as shown in Figure 11 on the right side. This was also consistent with the multilayer membrane structure model described by Machado *et al.*[32] He proposed that for small solvent concentrations in the coagulation bath, the precipitation rate of the sublayer adjacent to the surface increased. Because of this acceleration, a more

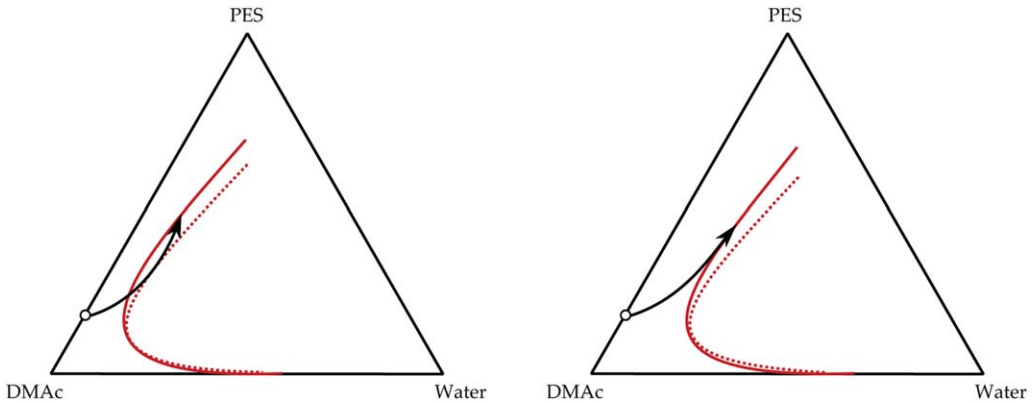

Figure 11. Schematic of the process. The left side shows no ethanol and instantaneous demixing. The right side shows the ethanol shifting the curves to the right and delayed demixing. The arrowhead marks the top of the film, and the point marks the bottom. In the left part, the layers below the top immediately formed the membrane, whereas in the right part, this was not the case. The picture was adapted and modified from ref. 26. Copyright 1996 Dordrecht. [Color figure can be viewed in the online issue, which is available at wileyonlinelibrary.com.]

porous sublayer was formed; this resulted in an increased PWF of the membrane. With increased additive in the coagulation bath, the effect of delayed demixing dominated, and this led to denser membranes and a reduction in the PWF. This effect is shown clearly in Figure 8.

To verify the reasoning brought forth here, control experiments with isopropyl alcohol and acetone, respectively, were undertaken. When the argumentation held, the effect of the ethanol should have only been an entropic one, and the nature of the diluent should not have been of significance. This was actually observed for all of the three organic additives (see Figure 8). However, this led to the assumption that all organic additives with negligible interactions should have shown the same behavior, where only the amount and not the nature of the additive played a role. Thus, the effect based on the entropic influence was a colligative one (in analogy to the cryoscopic effect of, e.g., salts).

Furthermore, the region where the composition path was in the metastable regime between the binodal and spinodal curve was enlarged; when the curves were shifted to the right, this could, in theory, lead to a higher statistical nature of the process, that is, larger error bars in the experiments. This was, in fact, clearly observed, as a multitude of experiments ($n = 13$ for each system) were undertaken with pure water and a water–ethanol mixture of 10% ethanol. The coefficient of variation increased from 4% (mean = 978.5 and $\sigma = 39.1$ L m^{-2} h^{-1}, where σ is standard deviation) for pure water to 19% (mean = 1284.9 and $\sigma = 243.9$ L m^{-2} h^{-1}) for 10% ethanol in the nonsolvent.

CONCLUSIONS

Flat-sheet membranes with different PES contents were prepared by a phase-inversion process with various amounts of additives (ethanol, acetone, and isopropyl alcohol) in the nonsolvent bath. On average, six membranes for each composition were produced to ensure statistical significance. The effects of the coagulation medium mixture on the cloud-point position, membrane morphology, PWF, and macromolecule retention were investigated. The results from cloud-point determination indicated that the demixing gap decreased with increasing additive content. This signified a trend in the delayed onset of liquid–liquid demixing. This was in accordance with the discussed thermodynamic considerations. Denser membrane structures were observed in an SEM study for ethanol, acetone, and isopropyl alcohol. These results correlated with the PWF obtained from filtration experiments. An addition of 10% additive led to an increase in the flux, whereas higher additive concentrations resulted in a reduction of the water flux. In other words, small values of ethanol, acetone, and isopropyl alcohol increased the permeability values of the PES membranes. With extended additive values, delayed demixing was increased, and the resulting membranes were less porous. The results from macromolecular rejection show that the membranes prepared with 10% additive in the water bath had a lower dextran retention compared to membranes formed in pure water. The data indicated that a further increase in the additive amount led to a decrease in *R*. Different results were obtained when we looked at gas-permeation membranes as Moradihamedani *et al.*[12] pointed out that different solubility parameters caused distinct differences in the performance and morphology. The difference may have been caused, on the one hand, by different applications (gas vs liquid separation) and formation process (no PVP was used). On the other hand, the morphology was a highly kinetically controlled phenomenon, and Sadrzadeh and Bhattacharjee[33] suggested that the properties of the formed membranes are often a fragile balance between thermodynamic enhancement and kinetic properties. Some information about the phase-inversion kinetics could, in fact, be drawn from the data. For example, as shown in Figure 8, at 10% additive concentration, the PWF was the highest for ethanol, followed by acetone and isopropyl alcohol. This was consistent with the sequence of molar volumes (with ethanol having the smallest and isopropyl alcohol having the largest). As Madaeni and Moradi[15] pointed out, increasing molar volume should correlate with increasing top-layer thickness (because of the lower diffusion rate). This should, in turn, have resulted in a lower PWF. Furthermore, the system was actually a quintary system (PES, PVP, water, DMAc, and various organic additives) reduced to a ternary one for the sake of simplicity. This simplification was justified by the experimental results, which show little difference in the separation behavior for the various additives used. Nevertheless, a quantitative theoretical approach was desirable. It has to be stressed again that the reasoning brought forth here is only of a thermodynamic nature, and it neglects kinetic behavior. Further theoretical in-depth studies might be a fruitful task and might elucidate this complex system in the future.

ACKNOWLEDGMENTS

The authors sincerely thank Sparkling Science (SPA/03-16) for its financial support of this project.

REFERENCES

1. Loeb, S.; Sourirajan, S. Saline Water Conversion II; Advances in Chemistry Series 38; American Chemical Society: Washington, DC, **1963**; p 117.
2. Reuvers, A. J.; van den Berg, J. W. A.; Smolders, C. A. *J. Membr. Sci.* **1987**, *34*, 45.
3. Young, T. H.; Chen, L. W. *J. Membr. Sci.* **1991**, *59*, 169.
4. Ren, J.; Li, Z.; Wong, F. S.; Li, D. *J. Membr. Sci.* **2005**, *248*, 177.
5. Young, T. H.; Chen, L. W. *J. Membr. Sci.* **1991**, *57*, 69.
6. Ulbricht, M. *Polymer* **2006**, *47*, 2217.
7. Al Malek, S. A.; Abu Seman, M. N.; Johnson, D.; Hilal, N. *Desalination* **2012**, *288*, 31.
8. Matsuyama, H.; Maki, T.; Teramoto, M.; Kobayashi, K. *Sep. Sci. Technol.* **2003**, *38*, 3449.
9. Wu, L.; Sun, J.; He, C. *J. Appl. Polym. Sci.* **2010**.
10. Madaeni, S. S.; Enayati, E.; Vatanpour, V. *J. Appl. Polym. Sci.* **2011**, *122*, 827.
11. Chun, K. Y.; Jang, S. H.; Kim, H. S.; Kim, Y. W.; Han, H. S.; Joe, Y. *J. Membr. Sci.* **2000**, *169*, 197.

12. Moradihamedani, P.; Ibrahim, N. A.; Yunus, W. M. Z. W.; Yusof, N. A. *J. Appl. Polym. Sci.* **2013**, *130*, 1139.
13. Iqbal, M.; Man, Z.; Mukhtar, H.; Dutta, B. K. *J. Membr. Sci.* **2008**, *318*, 167.
14. Smolders, C. A.; Reuvers, A. J.; Boom, R. M.; Wienk, I. M. *J. Membr. Sci.* **1992**, *73*, 259.
15. Madaeni, S. S.; Moradi, P. *J. Appl. Polym. Sci.* **2011**, *121*, 2157.
16. Wijmans, J. G.; Kant, J.; Mulder, M. H. V.; Smolders, C. A. *Polymer* **1985**, *26*, 1539.
17. Shirazi, M.; Kargari, A.; Bazgir, S.; Tabatabaei, M.; Shirazi, M.; Abdullah, M. S.; Matsuura, T.; Ismail, A. F. *Desalination* **2013**, *329*, 1.
18. Shirazi, M. M. A.; Bastani, D.; Kargari, A.; Tabatabaei, M. *Desalination Water Treatment* **2013**, *51*, 6003.
19. Wang, D.; Li, K.; Teo, W. K. *J. Membr. Sci.* **1996**, *115*, 85.
20. Baker, R. W. Membrane Technology and Applications; McGraw-Hill: New York, **2000**.
21. Kesting, R. E. Synthetic Polymeric Membranes: A Structural Perspective; Wiley: New York, **1985**.
22. Mulder, M. H. V.; Oude Hendrikman, J.; Wijmans, J. G.; Smolders, C. A. *J. Appl. Polym. Sci.* **1985**, *30*, 2805.
23. Feng, X.; Guo, Y.; Chen, X.; Zhao, Y.; Li, J.; He, X.; Chen, L. *Desalination* **2012**, *290*, 89.
24. Deshmukh, S. P.; Li, K. *J. Membr. Sci.* **1998**, *150*, 75.
25. Ahmad, A. L.; Ramli, W. K. W.; Fernando, W. J. N.; Daud, W. R. W. *Sep. Purif. Technol.* **2012**, *88*, 11.
26. Mulder, M. Basic Principles of Membrane Technology; Springer: Dordrecht, The Netherlands, **1996**.
27. Hansen, C. M. Hansen Solubility Parameters: A User's Handbook; CRC: Boca Raton, FL, **2007**.
28. Reuvers, A. J. Ph.D. Thesis, University of Twente, Netherlands, **1987**.
29. Wang, D.; Li, K.; Teo, W. K. *J. Membr. Sci.* **1998**, *138*, 193.
30. Barzin, J.; Sadatnia, B. *J. Membr. Sci.* **2008**, *325*, 92.
31. Barzin, J.; Sadatnia, B. *Polymer* **2007**, *48*, 1620.
32. Machado, P. S. T.; Habert, A. C.; Borges, C. P. *J. Membr. Sci.* **1999**, *155*, 171.
33. Sadrzadeh, M.; Bhattacharjee, S. *J. Membr. Sci.* **2013**, *441*, 31.